Cavity-enhanced optical bistability of Rydberg atoms

Qinxia Wang,[1,2] Zhihui Wang,[1,2] Yanxin Liu,[1,2] Shijun Guan,[1,2] Jun He,[1,2] Chang-Ling Zou,[1,3] [iD] Pengfei Zhang,[1,2] [iD] Gang Li,[1,2,*] [iD] and Tiancai Zhang[1,2]

[1]*State Key Laboratory of Quantum Optics and Quantum Optics Devices, Institute of Opto-Electronics, Shanxi University, Taiyuan 030006, China*
[2]*Collaborative Innovation Center of Extreme Optics, Shanxi University, Taiyuan 030006, China*
[3]*CAS Key Laboratory of Quantum Information, University of Science and Technology of China, Hefei, Anhui 230026, China*
*gangli@sxu.edu.cn

Optical bistability (OB) of Rydberg atoms provides a new, to the best of our knowledge, platform for studying nonequilibrium physics and a potential resource for precision metrology. To date, the observation of Rydberg OB has been limited in free space. Here, we explore cavity-enhanced Rydberg OB with a thermal cesium vapor cell. The signal of Rydberg OB in a cavity is enhanced by more than one order of magnitude compared with that in free space. The slope of the phase transition signal at the critical point is enhanced more than 10 times that without the cavity, implying an enhancement of two orders of magnitude in the sensitivity for Rydberg-based sensing and metrology. © 2023 Optica Publishing Group

Optical bistability (OB) of Rydberg atoms provides an interesting platform to study nonequilibrium physics [1–3] and embraces important applications [4,5]. Owing to the large dipole moments and strong interatomic interactions [6] associated with Rydberg atoms [7,8], the OB can be directly observed in free space. The feedback is applied by the generally assumed dipole–dipole interactions [1,9]. However, recent research shows that it could also be caused by ion-induced Stark shift [10,11]. To date, the Rydberg OB has been studied only in free space [1,3–5,9,10,12]. Moreover, recently, Ding and his colleagues studied the nonequilibrium phase transition and observed signatures of self-organized criticality [3] in a thermal vapor of atoms being optically excited to a strongly interacting Rydberg state. They further proposed and experimentally tested sensitivity-enhanced metrology at the critical point of the OB transition [5]. Benefiting from the many-body effects, the experiment showed three orders of magnitude improvement in the measurement precision of the microwave (MW) electric fields. The precision is limited by the maximum slope of the OB signal in the Rydberg excitation.

The optical cavity can enhance the light–matter interaction [13,14] and has been adopted in many experiments to improve the precision of measurement [15] or induce long-range interaction between atoms [16–20]. The OB of atoms with low energy states can also be observed through electromagnetically induced transparency (EIT) with the aid of an optical cavity [21–25]. In this Letter, we investigate the OB of Rydberg atoms in an optical cavity. The results show that the OB signal of the Rydberg atoms can be dramatically enhanced by the cavity. The slope of the phase transition edge at the critical point can be increased more than 10 times, implying a two orders of magnitude precision enhancement for Rydberg-based sensing and metrology.

First, the difference between free space and cavity-enhanced EIT and OB based on the Rydberg atoms is discussed from a theoretical perspective. In both configurations, three-level atoms are interacting with two laser beams and the corresponding energy diagram is shown in Fig. 1(a), which is widely adopted in Rydberg EIT and OB research. The three atomic states are the ground state $|g\rangle$, excited state $|e\rangle$, and Rydberg state $|r\rangle$. A probe (coupling) laser couples atomic transition $|g\rangle \rightarrow |e\rangle$ ($|e\rangle \rightarrow |r\rangle$) with Rabi frequency Ω_p (Ω_c) and frequency detuning Δ_p (Δ_c), where Γ_r is the decay rate from the Rydberg state $|r\rangle$, and Γ_e is the decay rate from the excited state $|e\rangle$. A transmission spectrum of the probe laser, obtained by scanning the frequency of the coupling laser, is often extracted to study the Rydberg EIT [26–30] and OB [1,3–5,9,10]. The EIT spectrum can be theoretically obtained by modeling the system via complete optical Bloch equations (OBEs) [3]. The interaction between Rydberg atoms is included by the replacement $\Delta_c \rightarrow \Delta_c + \Delta'$, with Δ' the frequency shift of Rydberg atoms. We also have $\Delta' = V \times \rho_{rr}$ with ρ_{rr} the population of the Rydberg state $|r\rangle$ and V the interaction-shift coefficient.

By solving master equations in the steady-state condition, we obtain the atomic susceptibility

$$\chi = -\frac{Nu_{ge}^2}{\varepsilon_0 \Omega_p} \rho_{ge}, \tag{1}$$

where N is the density of atoms; u_{ge} is the transition dipole moment; and ε_0 is the dielectric constant. The imaginary and real parts of the susceptibility, Im(χ) and Re(χ), represent, respectively, the absorption and dispersion of the probe laser. Thus, for the free space case, the transmission of the probe laser through the medium is

$$T_F = e^{-k_p l \text{Im}(\chi)}, \tag{2}$$

where k_p is the wave vector of the probe laser and l is the length of the medium.

For the cavity-enhanced OB and EIT, a cavity on-resonance with the probe light is introduced and the atomic vapor is placed inside, as shown in Fig. 1(b). The corresponding transmission
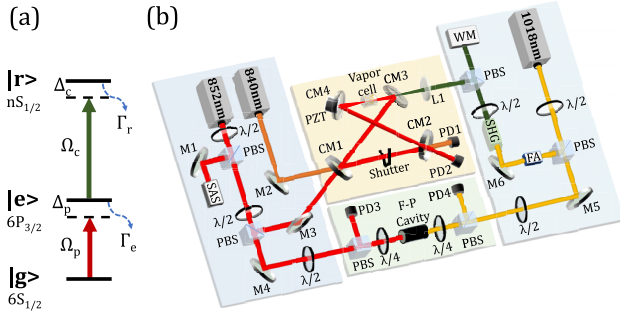
Fig. 1. (a) Energy level scheme used in both theory and experiment. (b) Experimental setup: CM, cavity coupler; FA, fiber amplifier; F-P cavity, Fabry–Pérot cavity; L, lens; M, mirror; PBS, polarization beam splitter; PD, photodiode; PZT, piezoelectric transducer; SAS, saturation absorption spectroscopy; SHG, second harmonic generation; shutter, optical shutter; WM, wave meter; $\lambda/2$, half-wave plate; $\lambda/4$, quarter-wave plate.

Fig. 2. Theoretical model for transmission spectra (a) without and (b) with consideration of Rydberg interaction. The spectra of the atom vapor in the cavity and free space are shown as black and red lines. The blue dashed lines and numbers show the maximum slopes k near the half transmission as indicated by points P_1 (cavity) and P_2 (free space). In (b), the Rydberg interaction with $V/2\pi = -100\,\text{MHz}$ is taken into account so that OB (phase transition) appears. The OB width in the free space and cavity are $2\pi * 11.6\,\text{MHz}$ and $2\pi * 12\,\text{MHz}$, respectively. The transmissive intensity (left axis) is normalized to the baseline of the signal (level far off from the resonance), and the peak height (right axis) is normalized to the height of the peak in free space. The parameters for the calculations are: $N = 5 \times 10^8 \text{cm}^{-3}$, $l = 10$ mm, $\Omega_p/2\pi = 13$ MHz, $\Omega_c/2\pi = 13$ MHz, $\Gamma_e/2\pi = 5.2$ MHz, $\Gamma_r/2\pi = 3$ MHz, $R_1 = 0.95$, $R_2 = 0.98$.

of the probe beam through the cavity–atom system has the following form [31]:

$$T_C = \frac{T_1 T_2}{1 + R_1 R_2 T_F^2 - 2\sqrt{R_1 R_2}\, T_F \cos(wl\,\text{Re}(\chi)/2c)}, \quad \textbf{(3)}$$

where T_1 (T_2) and R_1 (R_2) are the transmissivity and reflectivity of the input (output) mirror, respectively. The transmission spectra can be analyzed by using Eq. (3). According to Eq. (2), the transmission of a free space Rydberg atomic ensemble is determined only by $\text{Im}(\chi)$. However, the transmission of a cavity–atom system is determined by both $\text{Im}(\chi)$ and $\text{Re}(\chi)$; $\text{Im}(\chi)$ changes the intracavity losses and then affects the impedance mode matching of the cavity, and $\text{Re}(\chi)$ alters the dispersion of the cavity.

A comparison of the transmission spectra with and without the cavity, which are calculated according to experimentally feasible parameters, is shown in Fig. 2. Here, the frequency of the probe laser is fixed at $\Delta_p = 0$, and the frequency of the coupling laser Δ_c is scanned. To quantitatively compare the results, we deliberately set the intracavity circulating intensity (with cavity) and propagating intensity in free space (without cavity) of the probe laser with the same Rabi frequency at the frequency far off from the resonance. When the Rydberg interaction is absent, i.e., $V = 0$, both spectra show standard Lorentz shapes, as shown in Fig. 2(a). The enhancement of the cavity is obvious in that the amplitude of the transmission signal is enlarged by 10 times. This enhancement mainly comes from the improvement of the impedance mode matching [32] of the probe laser coupling into the cavity mode, owing to the change in $\text{Im}(\chi)$ at the double-resonance condition. When the Rydberg interaction is considered, the typical hysteresis OB signal with Δ_c scanned is observed [Fig. 2(b)]. Here, not only the amplitude of the OB signal but also the width of the OB is enlarged by the cavity. The reason for the enhancement of the amplitude is the same as in the case without Rydberg interaction, and the reason for the enhancement of the OB width is the consequent boost of both the population and Rydberg interaction of state $|r\rangle$. The enhancement of OB width and amplitude will be eventually saturated as the Rydberg excitation keeps increasing.

In the scenario of the precision measurement of the MW electric fields by Rydberg atoms, a steeper slope of the spectrum is
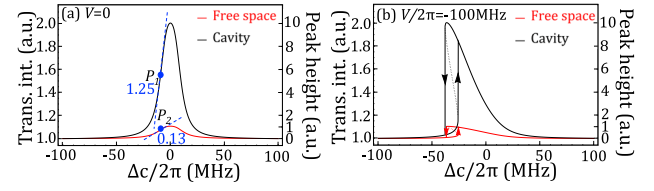
desired because it indicates a better measurement sensitivity. The critical point of the phase transition due to the many-body Rydberg interaction has been proven to enhance the precision by three orders of magnitude [5]. Therefore, the cavity-enhanced Rydberg signal implies a potential improvement in future applications. To show this point, the maximum slopes of the spectra in Fig. 2(a) (shown as the dashed lines) are extracted. It is evident that, by using the cavity, the measurement precision can be enhanced by approximately one order of magnitude due to a higher transmittance. However, the value of slopes could not be determined in Fig. 2(b) because the nonequilibrium dynamics of the OB at the critical point cannot be obtained from a steady-state solution. In practice, the slope is related to the laser's sweeping speed and the system's relaxation and could be determined in the following experiments. Nevertheless, it is anticipated that the slope at the critical point of the cavity-enhanced OB is significantly enhanced due to its larger amplitude. The enhancement is roughly proportional to the cavity finesse, with a coefficient of approximately 0.56.

The cavity-enhanced Rydberg OB is investigated experimentally with a cesium (Cs) atomic vapor cell. The atomic energy levels and the layout of the experimental setup are shown in Fig. 1. The key device is an optical bow-tie cavity composed of four cavity mirrors, two flat mirrors (CM1 and CM2), and two plano–concave mirrors (CM3 and CM4) with a radius of curvature of 100 mm. CM3 and CM4 are separated by approximately 120 mm, with a total cavity length of approximately 480 mm. Therefore, the primary mode waist resides between CM3 and CM4 with a size of 50 µm, where a thermal Cs vapor cell with a length of 10 mm and temperature of 30°C is placed. CM1 (with a transmissivity of 5% at 852 nm) and CM2 (with a transmissivity of 2% at 852 nm) serve as input and output couplers, respectively. CM3 and CM4 are coated with high reflectivity (>99.9%) at 852 nm and high transmissivity (~90%) at 509 nm. The finesse of the empty cavity is approximately 85, which is reduced to approximately 20 when the vapor cell is counted, owing to the atom absorption and the reflection of the cell walls. The cavity length is stabilized by a piezoelectric transducer (PZT) mounted

on CM4, which is achieved through an auxiliary locking beam from a frequency-stabilized 840-nm diode laser.

Rydberg excitation is achieved by two lasers, as shown in Fig. 1(a). The probe laser is an 852-nm laser, which is injected from input coupler CM1 to resonantly drive the Cs atomic transition from the ground state $|g\rangle = |6S_{1/2}, F = 4\rangle$ to the excited state $|e\rangle = |6P_{3/2}, F' = 5\rangle$. The probe laser frequency is referenced to the saturated absorption spectroscopy (SAS) of another Cs vapor, and the cavity mode is tuned to be on-resonance with the probe laser to enhance the intracavity laser intensity. The coupling laser is a 509-nm laser, which is generated by frequency doubling (second harmonic generation, SHG) of an amplified fundamental 1018-nm laser via a fiber amplifier (FA). The coupling laser is injected from coupler CM3, and the waist is transformed to approximately 80 μm by lens L1. The coupling laser is scanned over the atomic transition from the excited state $|e\rangle = |6P_{3/2}, F' = 5\rangle$ to the Rydberg state $|r\rangle = |51S_{1/2}\rangle$ and the frequency is monitored by a wavemeter. The frequencies of both lasers are stabilized to a stable high-finesse Fabry–Pérot (F-P) cavity, which serves as a frequency standard, via the Pound–Drever–Hall (PDH) technique.

In our experiments, the transmission spectra of the probe light with and without the cavity are recorded with the same experimental setup. The switching between free space and cavity-enhanced experimental configurations is achieved by an intracavity shutter, which is placed between CM1 and CM2. The spectra are measured by PD2 (C30659-900-R8A, Perkin Elmer). The typical Rydberg OB spectra with and without cavity are shown in Fig. 3. We can see that the peak height of the OB signal is enhanced by approximately 10 times with the optical cavity, which is consistent with the theory in Fig. 2 (b).

The spectra of the Rydberg OB are then studied for a series of Ω_p, with Ω_c being fixed, and the results are summarized in Fig. 4. In free space, the OB signal is invisible with a low probe light [as shown in Fig. 4(a6)] because of the low excitation of the Rydberg state ($\rho_{rr} \approx 0$), where the interaction between the atoms can be omitted. The excitation of the Rydberg state (ρ_{rr}) increases by enhancing Ω_p. Thus, the OB signal becomes visible, and the amplitude and width become increasingly larger, owing to the stronger Rydberg interaction. As a comparison, when using the cavity, the OB signals appear at a lower probe power [Fig. 4(b6)], by which the OB is invisible in free space. These results are consistent with the theory, and our theory predicts that the cavity enhances not only the OB amplitude but also the
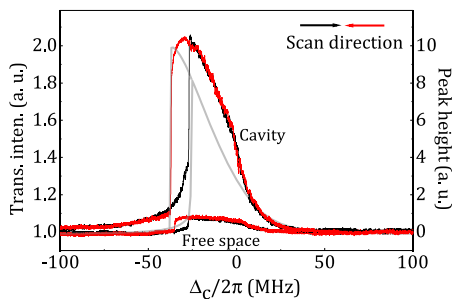

Fig. 4. Experimental results of Rydberg OB in: (a1) to (a6) free space; (b1) to (b6) cavity. Spectra taken with fixed Rabi frequency of coupling light, with $\Omega_c/2\pi = 20$ MHz and a series of probe light Rabi frequencies, $\Omega_p/2\pi$ of: (a6), (b6) 11 MHz; (a5), (b5) 17 MHz; (a4), (b4) 20 MHz; (a3), (b3) 24 MHz; (a2), (b2) 27 MHz; (a1), (b1) 30 MHz. The power of probe light in front of CM1 is displayed in each sub-figure in the small panel with black line. The spectra are obtained with the frequency of coupling light scanned (black curve) up and (red curve) down, with scanning speed $2\pi \times 0.01$ MHz/μs. The spectra are shown as both the transmissive intensity [normalized to level of baseline in (a6)] of the probe light versus Δ_c (left axis). The numbers associated with the dashed lines are the maximum slopes k at the critical points. The variance of the noise associated with each spectrum is also indicated as Var(μ), which is the mean square root of the fluctuations and normalized to the baseline of (a6).

Fig. 3. Experimental results of Rydberg OB in free space and cavity: spectra taken with same Rabi frequencies of coupling and probe lights, $\Omega_c/2\pi = \Omega_p/2\pi = 13$ MHz. Black curve: frequency of coupling light scanned up. Red curve: frequency of coupling light scanned down. Transmissive intensity is normalized to level of baseline of probe light. Light gray curve: theoretical prediction of cavity-enhanced Rydberg OB.
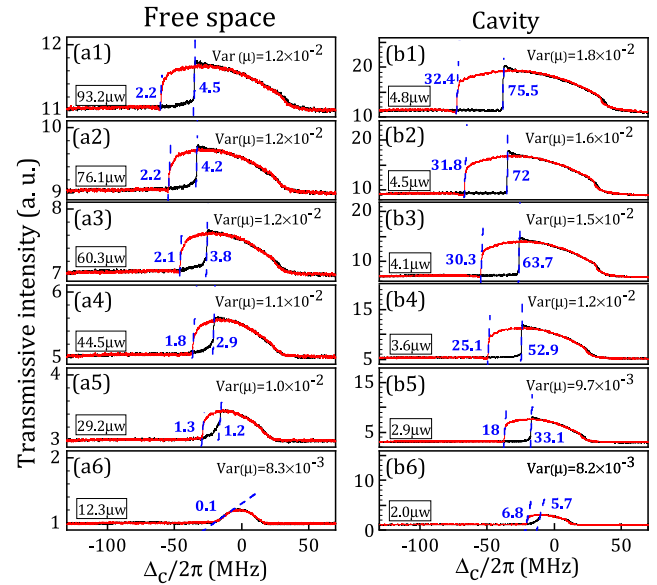
OB frequency shift and width, compared with the cases in free space.

The maximum slope k of the OB spectra at the critical point provides a potential approach for measuring the MW electric field [5]. As discussed, steady-state semiclassical theory cannot give direct evidence for the enhancing effect of the slope by using the cavity. Here, we extracted the value of k for each spectrum and marked it in Fig. 4. The variances of the noise associated with the spectra are also measured and shown as Var(μ) in each sub-figure. We found that, compared with the maximum slope without OB [Fig. 4(a6)], k is enhanced by more than 10 times on average (45 times at most) with the OB in free space [Figs. 4(a2) to 4(a6)]. The noise is enlarged only approximately 1.5 times at most. These results agree well with Ding *et al.* [5]. By adopting the cavity, k is further enhanced by approximately 15 times, and the noise is enlarged by another 1.2 on average (1.5 times at most). The enlarged noise mainly comes from the instability of the cavity, which is determined by the cavity-locking loops. The noise could be suppressed further by optimizing the locking loop.

Fisher information (FI) is a figure of merit to evaluate the sensitivity of the measurement. According to Ding *et al.* [5], the enhancement ratio for FI can be calculated as $(k^2/\text{Var}(\mu))/(k_0^2/\text{Var}(\mu_0))$, in which k and k_0 are the slopes of the
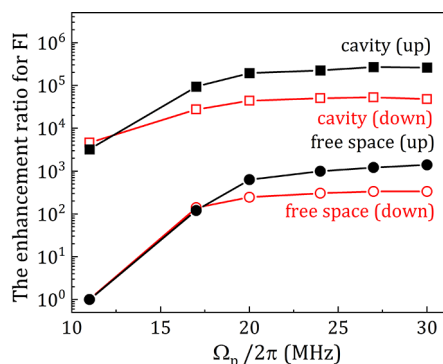
Fig. 5. Enhancement ratio for FI versus Rabi frequency of probe light. The enhancement ratio for FI is calculated from the maximum slope k and noise level Var(μ) associated with OB in Fig. 4 and those associated with the Rydberg EIT [Fig. 4(a6)]. Up and down in parentheses denote scanning directions of coupling light frequency to obtain spectra.

---

two spectra and Var(μ) and Var(μ_0) are the associated noise levels, respectively. The enhancement ratio for FI of every spectrum with OB in Fig. 4 over the Rydberg EIT [Fig. 4(a6)] is calculated and summarized in Fig. 5. It is clear that the FI, as well as the measurement sensitivity, can be enhanced by three orders of magnitude with OB in free space, which has been shown in Ding *et al.* [5]. Here, by using a cavity, the maximum slope k of OB can be improved by 750 times, whereas the FI can be enhanced by 10^5 compared with the free space Rydberg EIT, which is two orders of magnitude above that obtained from the OB in free space [5].

In summary, we studied the cavity-enhanced OB of the Rydberg atomic ensemble in both theory and experiment. To the best of our knowledge, this is the first time that the Rydberg-induced nonlinear OB effect has been studied experimentally within an optical cavity. We observed a more than 10-fold enhancement of the OB spectrum in a cavity than in free space. At the same time, improvements in the OB frequency shift, width, and threshold were also observed. Our experiments also show that the slope of the spectrum at the critical point can be enhanced by 15 times, and the FI can be enhanced by another two orders of magnitude. Therefore, the measurement sensitivity of the MW field could be significantly improved by using the cavity-enhanced Rydberg OB effect. This also provides a new platform for the study of nonequilibrium many-body systems with both short-range Rydberg interactions and long-range cavity-mediated interactions.

Disclosures. The authors declare no conflicts of interest.

Data availability. Data underlying the results presented in this paper are not publicly available at this time but may be obtained from the authors upon reasonable request.

REFERENCES

1. C. Carr, R. Ritter, C. G. Wade, C. S. Adams, and K. J. Weatherill, Phys. Rev. Lett. **111**, 113901 (2013).
2. M. Marcuzzi, E. Levi, S. Diehl, J. P. Garrahan, and I. Lesanovsky, Phys. Rev. Lett. **113**, 210401 (2014).
3. D.-S. Ding, H. Busche, B.-S. Shi, G.-C. Guo, and C. S. Adams, Phys. Rev. X **10**, 021023 (2020).
4. J. He, X. Wang, X. Wen, and J. Wang, Opt. Express **28**, 33682 (2020).
5. D.-S. Ding, Z.-K. Liu, B.-S. Shi, G.-C. Guo, K. Mølmer, and C. S. Adams, Nat. Phys. **18**, 1447 (2022).
6. T. Baluktsian, B. Huber, R. Löw, and T. Pfau, Phys. Rev. Lett. **110**, 123001 (2013).
7. C. S. Adams, J. D. Pritchard, and J. P. Shaffer, J. Phys. B: At., Mol. Opt. Phys. **53**, 012002 (2020).
8. M. Saffman, T. G. Walker, and K. Mølmer, Rev. Mod. Phys. **82**, 2313 (2010).
9. N. R. de Melo, C. G. Wade, N. Šibalić, J. M. Kondo, C. S. Adams, and K. J. Weatherill, Phys. Rev. A **93**, 063863 (2016).
10. D. Weller, A. Urvoy, A. Rico, R. Löw, and H. Kübler, Phys. Rev. A **94**, 063820 (2016).
11. D. Weller, J. P. Shaffer, T. Pfau, R. Löw, and H. Kübler, Phys. Rev. A **99**, 043418 (2019).
12. T. E. Lee, H. Häffner, and M. C. Cross, Phys. Rev. Lett. **108**, 023602 (2012).
13. H. J. Kimble, Phys. Scr. **T76**, 127 (1998).
14. S. M. Dutra, *Cavity Quantum Electrodynamics* (John Wiley and Sons, Ltd., 2004).
15. G. Gagliardi and H.-P. Loock, *Cavity-Enhanced Spectroscopy and Sensing* (Springer-Verlag, 2014).
16. S. Schütz and G. Morigi, Phys. Rev. Lett. **113**, 203002 (2014).
17. P. Münstermann, T. Fischer, P. Maunz, P. W. H. Pinkse, and G. Rempe, Phys. Rev. Lett. **84**, 4068 (2000).
18. E. J. Davis, G. Bentsen, L. Homeier, T. Li, and M. H. Schleier-Smith, Phys. Rev. Lett. **122**, 010405 (2019).
19. J. Muniz, D. Barberena, R. J. Lewis-Swan, D. J. Young, J. R. K. Cline, A. M. Rey, and J. K. Thompson, Nature **580**, 602 (2020).
20. A. Periwal, E. S. Cooper, P. Kunkel, J. F. Wienand, E. J. Davis, and M. Schleier-Smith, Nature **600**, 630 (2021).
21. A. Szöke, V. Daneu, J. Goldhar, and N. A. Kurnit, Appl. Phys. Lett. **15**, 376 (1969).
22. W. Harshawardhan and G. S. Agarwal, Phys. Rev. A **53**, 1812 (1996).
23. H. Wang, D. J. Goorskey, and M. Xiao, Phys. Rev. A **65**, 011801 (2001).
24. A. Joshi, A. Brown, H. Wang, and M. Xiao, Phys. Rev. A **67**, 041801 (2003).
25. H. Wang, D. J. Goorskey, W. H. Burkett, and M. Xiao, Opt. Lett. **25**, 1732 (2000).
26. L. Zhang, S. Bao, H. Zhang, G. Raithel, J. Zhao, L. Xiao, and S. Jia, Opt. Express **26**, 29931 (2018).
27. J. He, Q. Liu, Z. Yang, Q. Niu, X. Ban, and J. Wang, Phys. Rev. A **104**, 063120 (2021).
28. H.-J. Su, J.-Y. Liou, I.-C. Lin, and Y.-H. Chen, Opt. Express **30**, 1499 (2022).
29. W. Li, J. Du, M. Lam, and W. Li, Opt. Lett. **47**, 4399 (2022).
30. J. Yao, Q. An, Y. Zhou, K. Yang, F. Wu, and Y. Fu, Opt. Lett. **47**, 5256 (2022).
31. J. Sheng, H. Wu, M. Mumba, J. Gea-Banacloche, and M. Xiao, Phys. Rev. A **83**, 023829 (2011).
32. J. H. Chow, I. C. M. Littler, D. S. Rabeling, D. E. McClelland, and M. B. Gray, Opt. Express **16**, 7726 (2008).